

O_h Five Degree-of-freedom Fundamental Zone Properties via Voronoi Fundamental Zone Framework: Supplementary Information

Sterling G. Baird^{a,*}, Eric R. Homer^a, David T. Fullwood^a, Oliver K. Johnson^a

^a*Department of Mechanical Engineering, Brigham Young University, Provo, UT 84602, USA*

Contents

S1 Fe Input Data Quality	1
S2 Gridded Sampling for Numerical Differentiation	2
S3 GBs Used for Path Visualization	4

S1. Fe Input Data Quality

Of the $\sim 60\,000$ ¹ GBs in [1], $\sim 10\,000$ GBs were repeats that were identified by converting to Voronoi fundamental zone grain boundary octonions and applying Voronoi fundamental zone repository function `avg_repeats.m`. In [1], mechanically selected GBs were those which involved sampling in equally spaced increments² for each five degree-of-freedom parameter, and a few thousand intentionally selected GBs (i.e. special GBs) were also considered. Of mechanically and intentionally selected GBs, 9170 and 112 are repeats, respectively, with a total of 2496 degenerate sets³ (see Figure S1 for a degeneracy histogram). Thus, on average there is a degeneracy of approximately four per set of degenerate GBs.

By comparing grain boundary energy values of (unintentionally⁴) repeated GBs in the Fe simulation dataset [1], we can estimate the intrinsic error of the input data. For example, minimum and maximum deviations from the average value of a degenerate set are -0.2625 J m^{-2} and 0.2625 J m^{-2} , respectively, indicating that a repeated Fe GB simulation from [1] can vary by as much as 0.525 J m^{-2} , though rare. Additionally, Root mean square error and mean absolute error values can be obtained within each degenerate set by comparing against the set mean. Overall root mean square error and mean absolute error are then obtained by averaging and weighting by the number of GBs in each degenerate set. Following this procedure, we obtain an average set-wise root mean square error and mean absolute error of $0.065\,29\text{ J m}^{-2}$ and $0.061\,90\text{ J m}^{-2}$, respectively, which is an approximate measure of the intrinsic error of the data. Figure S2 shows histograms and parity plots of the intrinsic error. The overestimation of intrinsic error mentioned in the main text (??) could stem from bias as to what type of GBs exhibit

*Corresponding author.

Email address: `ster.g.baird@gmail.com` (Sterling G. Baird)

¹The “no-boundary” grain boundaries (GBs) (i.e. GBs with close to 0 J m^{-2} grain boundary energy) were removed before testing for degeneracy.

²In some cases, this was equally spaced increments of the argument of a trigonometric function.

³A degenerate “set” is distinct from a Voronoi fundamental zone grain boundary octonion “set”, the latter of which is often used in the main text.

⁴To our knowledge, the presence of repeat GBs were not mentioned in [1] or [2]

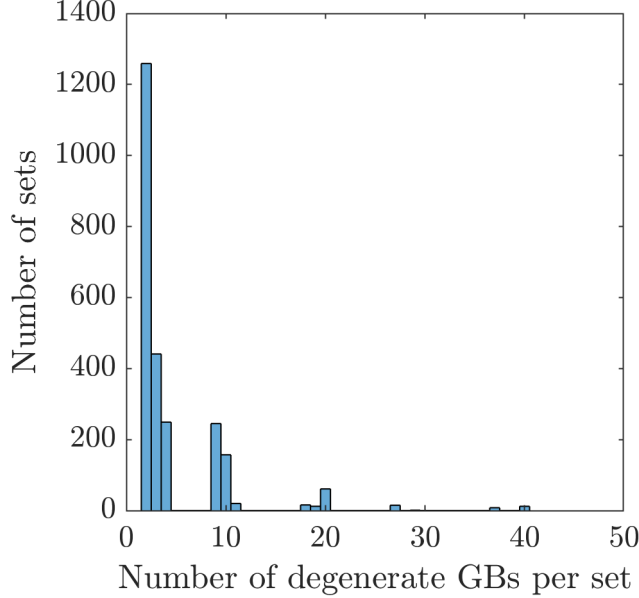


Figure S1: Histogram of number of sets vs. number of degenerate GBs per set for the Fe simulation dataset [1]. Most sets have a degeneracy of fewer than 5.

repeats based on the sampling scheme used in [1] and/or that many of the degenerate sets contain a low number of repeats (Figure S1).

Next, we see that by binning GBs into degenerate sets, most degenerate sets have a degeneracy of fewer than 5 Figure S1. We split the repeated data into sets with a degeneracy of fewer than 5 and greater than or equal to 5 and plot the errors (relative to the respective set mean) in both histogram form (Figure S2a and Figure S2c, respectively) and as hexagonally-binned parity plots (Figure S2b and Figure S2d, respectively). While heavily repeated GBs tend to give similar results, occasionally repeated GBs often have larger grain boundary energy variability. This could have physical meaning: Certain types of (e.g. high-symmetry) GBs tend to have less variation (i.e. fewer and/or more tightly distributed metastable states). However, it could also be an artifact of the simulation setup that produced this data (e.g. deterministic simulation output for certain types of GBs).

S2. Gridded Sampling for Numerical Differentiation

Related to Section 4.1, an isotropically sized fundamental zone may be easier to uniformly discretize than a high aspect-ratio space (i.e. a fixed discretization length can be used across all dimensions). What this doesn't describe, however, is curvature. In order to create a gridded array, which is important for numerical differentiation, a hypercube with each primary axis oriented with Euclidean dimensions is to be preferred. As curvature or misalignment is introduced as may be expected with a Voronoi fundamental zone point cloud, GBs outside of the Voronoi fundamental zone will necessarily be sampled; this phenomena will be exaggerated in high dimensions⁵. Fortunately, most of the information is contained

⁵For perspective, a discretization into 9 segments (10 points) along each dimension will have a spacing of $\sim 7^\circ$ and require 1×10^5 grid points. In order to achieve a more reasonable grid spacing of $\sim 2^\circ$, a minimum of ~ 24 discretizations (25 points) along each dimension is necessary and will produce $\sim 1 \times 10^7$ grid points.

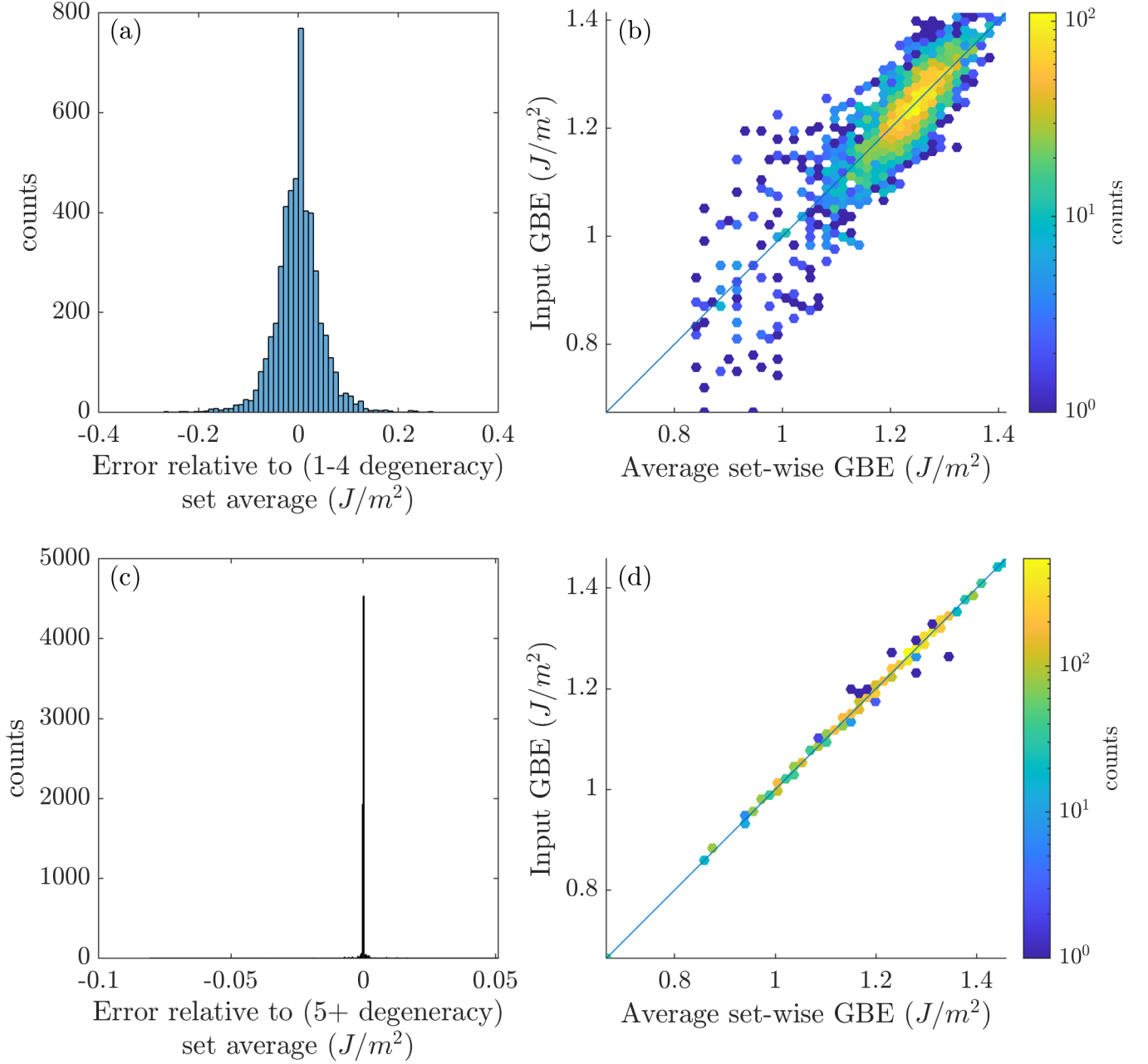


Figure S2: Degenerate GBs sets are split into those with a degeneracy of fewer than 5 and greater than or equal to 5 and plotted as (a) and (c), respectively) error histograms and (b) and (d), respectively) hexagonally-binned parity plots. Large degenerate sets tend to have very low error, whereas small degenerate sets tend to have higher error. In other words, GBs that are more likely to be repeated many times based on the sampling scheme in [1] tend to give similar results, whereas GBs that are less likely to be repeated often have larger variability in the simulation output. We do not know if this has physical meaning or is an artifact of the simulation setup.

in the first five dimensions after singular value decomposition transformation (Section 3.2). Thus, the latter three dimensions can likely be ignored without substantially affecting e.g. an interpolation or numerical differentiation scheme.

S3. GBs Used for Path Visualization

Table 1: Minimum Σ (Sigma) GBs and corresponding IDs used for path visualization within the original Olmsted et al. [3] dataset.

Sigma	Olmsted ID
3	3
5	169
7	32
9	21
11	33

Table 2: Minimum Σ (Sigma) GBs and corresponding IDs used for path visualization within the original Kim et al. [1] dataset.

Sigma	Kim Special ID
3	7
5	162
7	259
9	315
11	406

References

- [1] H.-K. Kim, S. G. Kim, W. Dong, I. Steinbach, B.-J. Lee, Phase-field modeling for 3D grain growth based on a grain boundary energy database, *Modelling and Simulation in Materials Science and Engineering* 22 (2014) 034004. doi:[10.1088/0965-0393/22/3/034004](https://doi.org/10.1088/0965-0393/22/3/034004).
- [2] H. K. Kim, W. S. Ko, H. J. Lee, S. G. Kim, B. J. Lee, An identification scheme of grain boundaries and construction of a grain boundary energy database, *Scripta Materialia* 64 (2011) 1152–1155. doi:[10.1016/j.scriptamat.2011.03.020](https://doi.org/10.1016/j.scriptamat.2011.03.020).
- [3] D. L. Olmsted, E. A. Holm, S. M. Foiles, Survey of computed grain boundary properties in face-centered cubic metals-II: Grain boundary mobility, *Acta Materialia* 57 (2009) 3704–3713. doi:[10.1016/j.actamat.2009.04.015](https://doi.org/10.1016/j.actamat.2009.04.015).